Contents lists available at ScienceDirect

Food Chemistry

Sourdough process and spirulina-enrichment can mitigate the limitations of colon fermentation performances of gluten-free breads in non-celiac gut model

Lorenzo Nissen [a,b,d,*], Flavia Casciano [a,d], Elena Chiarello [a], Mattia Di Nunzio [c], Alessandra Bordoni [a,b], Andrea Gianotti [a,b,d,*]

[a] *DiSTAL - Department of Agricultural and Food Sciences, Alma Mater Studiorum – University of Bologna, P.za G. Goidanich, 60, 47521 Cesena, Italy*
[b] *CIRI - Interdepartmental Centre of Agri-Food Industrial Research, Alma Mater Studiorum – University of Bologna, P.za G. Goidanich, 60, 47521 Cesena, Italy*
[c] *Department of Food, Environmental and Nutritional Sciences (DEFENS), University of Milan, via Celoria 2, 20133 Milan, Italy*
[d] *CRBA, Centre for Applied Biomedical Research, Alma Mater Studiorum - University of Bologna, Policlinico di Sant'Orsola, Bologna 40100, Italy*

ARTICLE INFO

ABSTRACT

In this work, the impact of gluten free (GF) breads enriched with spirulina on the ecology of the colon microbiota of non-celiac volunteers was investigated. Simulation of digestion of GF breads was conducted with an *in vitro* gut model. Microbiomics and metabolomics analyses were done during colon fermentations to study the modulation of the microbiota.

From the results, a general increase in *Proteobacteria* and no reduction of detrimental microbial metabolites were observed in any conditions. Notwithstanding, algae enriched sourdough breads showed potential functionalities, as the improvement of some health-related ecological indicators, like i) microbiota eubiosis; ii) production of bioactive volatile organic fatty acids; iii) production of bioactives terpenes. Our results indicate that a sourdough fermentation and algae enrichment can mitigate the negative effect of GF breads on gut microbiota of non-celiac consumers.

1. Introduction

Recently, the request for gluten-free (GF) food products has been increasing because of the growing gluten-related diseases, the improvement in detection rate of diagnoses, the induction of environmental factors (Aguiar et al., 2021; Zhang et al., 2022). Celiac disease (CD) is the most common gluten-related disease that occurs in genetically predisposed subject upon ingesting gluten-containing and the prevalence of CD based on serologic test results is 1.4 % worldwide (Scherf, 2019; Zhang et al., 2022). One of the main technological challenges in the production of gluten free bakery products is to improve their nutritional content, because common GF bakery products are nutritionally poor, for example in the content of proteins and bioactives. To unravel the issue, two feasible approaches could be the incorporation in the dough of an ulterior source of proteins and bioactives and the biotechnological transformation with fermentation. Otherwise, it is still problematic to produce high-quality leavened GF breads with non-wheat flour, due to difficulties to construct a continuous protein network by non-wheat proteins (Zhang et al., 2022). The seek for the right protein source is open and technologists have screened many different alternatives, as pseudocereals, legumes, nuts (Zhang et al., 2022), insects (Nissen et al., 2020) and lastly algae (Casciano et al., 2021) to include in GF bakery foods. Algae seems very promising as the proper way to drive protein enrichment in GF bakery, because are sustainable, rich in proteins and bioactives. For example, most of the biomass of the microalgae *Arthorospira platensis*, a.k.a. spirulina, being produced today is consumed as a nutritional supplement promoted as a "superfood" and sold as a dried powder, flakes, or capsules (Lafarga et al., 2020). Recently, either to improve the protein and the bioactives contents of GF bakery products, we have proposed the preparation and characterization of new GF breads formulated with *Arhtrospira platensis* powder (AP) and processed by sourdough fermentation. The product

obtained resulted to have a higher content in protein and bioactives and a prebiotic potential (Casciano et al., 2021). Another aspect to consider is that GF bakery products, even if are designed for specific consumers have a target audience that stretches beyond coeliac sufferers. For example, in the US in 2015, only 9 % of GF consumers were celiac sufferers, while the major part consumed GF foods because believe that are healthier products than the standard ones. This behavior is also called the "health halo" effect (Fradinho et al., 2020). Notwithstanding, it is not known which is the impact of specific foods on non-specific consumers, especially towards the gut microbiota.The gut microbiota is one of the principal human organs involved in the digestion of foods and that of celiac sufferers is adapted to the diseased condition and is trained in the digestion of GF foods, limiting ecological perturbations. Although, no data are available on how the microbiota of non-celiacs respond to GF products. In this sight it is necessary to understand the interaction among GF foods and the healthy human colon microbiota. To investigate and comprehend the mechanistic key role of food-microbes' interaction, before to set up a diet interventional trial or animal research, the use of *in vitro* intestinal model is the state of the science approach (Von Aulock, 2019). With this approach we can simulate on a bench under a hood laboratory the complex biological phenomena of food digestion of the whole gastro-intestinal human tract, from the oral cavity to the large intestine (Nissen, Casciano, et al. 2021). In this study, we employed a gut model based on healthy humans, coupling the INFOGEST static protocol, to simulate the oro-gastro-duodenal digestion (Minekus et al., 2014), to the colon model MICODE (Multi-Unit *in vitro* Colon Model), to simulate proximal colonic fermentation (Nissen, Casciano, et al. 2021; Nissen, Valerii, et al., 2021; Nissen et al. 2022, 2023). In the present work we tested GF breads made with and without protein enrichment by *Arthrospira platensis* powder (AP) and obtained by sourdough and plain (control) fermentations. Comparisons were observed after gastro-duodenal digestion and proximal colonic fermentation performed for a short-term experiment. The aim is to highlight and compare the impact of formulation and process of the breads on the human colon microbiota, throughout microbiomics (qPCR and 16S r-RNA MiSeq) and metabolomics (SPME GC–MS). Our principal hypothesis is that with a biotechnological transformation with spirulina enrichment and sourdough process of GF breads is possible to obtain a better product suitable also for non-celiac consumers. Also, the results of this work could serve to start to comprehend some key elements that stands behind the host-food interaction over the "health halo" effect.

2. Material and methods

2.1. Human colon microbiota

Human Colon Microbiota (HCM) was obtained from fecal samples of three lean healthy individuals. The number and type of volunteers, and the following procedures were in accordance with previous protocols (Arnal et al., 2021; Connolly et al., 2012; Nissen et al., 2023; Oba et al., 2020). Fecal donations were obtained from three healthy subjects, (either female and male) aged between 30 and 45 y. Donors did not undergo antibiotic treatment for at least 3 months prior to stool collection, did not intentionally consume pre- or probiotic supplements before the experiment, and had no history of bowel disorders. Additionally, the donors were not smokers, not chronically consuming any drug, and not alcoholic drink consumers. Fecal samples were donated two times (with an interval of seven days) for the two biological replicas. To collect feces, donors were provided and instructed to use a collection kit, which includes a stool collector (Sarstedt AG & Co. KG, Nümbrecht, Germany) and an anaerobic jar with a O_2 catalyst (Oxoid, Thermo Fisher Scientific, Waltham, MA, USA). Fecal samples were collected by volunteers in a dedicated sterile container, placed in an anaerobic jar with oxygen catalyst (Oxoid, Thermo Fisher Scientific, USA), transferred to the laboratory, and processed within 2 h. HCM was obtained by homogenizing 2 g of each donation in 54 mL of pre-reduced phosphate buffered saline (PBS) (Nissen et al., 2022; Wang et al., 2020). The three healthy donors were told of the study's aims and procedures and gave their verbal consent to use their feces for the experiments, in agreement with the ethics procedures required at the University of Bologna.

2.2. Experimental samples and controls

Experimental gluten free algae-enriched and control breads, traditionally processed (6 h of leavening with baker's yeast) and processed by sourdough (24 h of leavening with baker's yeast and a mix of lactic acid bacteria) were previously prepared and characterized (Casciano et al., 2021). From this previous characterization, it has emerged that the algae-enriched breads exert a strong prebiotic activity by means of culturomics. The gluten free bread samples tested in the present work were: AS = Algae-enriched breads sourdough processed; AT = Algae-enriched breads traditionally processed; CS = Control breads sourdough processed; CT = Control breads traditionally processed.

2.3. In vitro digestion and fermentation

Gluten free algae-enriched and control breads were digested *in vitro* with the INFOGEST protocol (Minekus et al., 2014). Digestates were then stored at −80 °C. Prior to *in vitro* colonic fermentation, the digestates were thawed and gently centrifuged to separate the dense portion, to be applied then *in vitro* fermentation. Short-term batch proximal colon fermentations were conducted for 24 h in independent vessels using an *in vitro* colon model, MICODE (Nissen, Casciano, et al. 2021; Nissen et al. 2022, 2023). The preparation of the experiments was made according to published procedures (Connolly et al., 2012; Wang et al., 2020) and was previously described in detail (Nissen, Casciano, et al. 2021; Nissen et al. 2022, 2023). Briefly, fermentation vessels were filled aseptically with 90 mL of basal medium (BM) (Connolly et al., 2012) and left running to reach and maintain the proximal colon ecological conditions (0.0 % of DO_2 and pH 5.75). Anaerobic condition (0.0–0.1 % w/v of DO_2) in each bioreactor was obtained in about 30 min flushing with filtered O_2-free N_2 through the mounted-in sparger of Minibio reactors (Applikon Biotechnology BV, NL), and was constantly kept over the experiment. Temperature was set at 37 °C and stirring at 300 rpm, while pH was adjusted to 6.75 and kept throughout the experiment with the automatic addition of filtered NaOH or HCl (0.5 M) to mimic the conditions located in the distal region of the human large intestine. Once the exact environmental settings were reached, the four vessels were aseptically injected with 10 mL of fecal slurry (10 % w/v of human feces to a final concentration of 1 %, w/v) and then four of them independently with 1 g of AT, AS, CT, or CS (to a final concentration of 1 %, w/v), while the fifth vessel was set as blank control (BC, basal medium and 1 % fecal slurry only). Batch cultures were run under these controlled conditions for a period of 26.02 ± 0.18 h during which samples were collected at 3 time points (baseline, 18, and 24 h). The baseline (BL), i.e., the period of adaptation of the human colon microbiota to the *in vitro* condition was defined on the first pH changes detected by Lucullus (1 read/10 s) via the pH Sensors of MICODE (Applisense, Applikon Biotechnology, BV, NL) and was set after 2.02 ± 0.18 h. Sampling was performed with a dedicated double syringe filtered system (Applikon Biotechnology BV, NL) connected to a float drawing from the bottom of the vessels without perturbing or interacting with the bioreactor's ecosystem. To guarantee a close control, monitoring and recording of fermentation parameters the software Lucullus 3.1 (PIMS, Applikon Biotechnology BV, NL) was used. This also allowed to keep the stability of all settings during the experiment. Fermentations were conducted in duplicate independent experiments, using for each a new pool of feces from the same three healthy donors.

2.4. Pipeline of experimental activities

Parallel and independent vessels for AT, AS, CT, CS, and BC were run

for 24 h after the adaptation of the fecal inoculum, defined as the BL. The entire experiment was based on 5 theses and 3 time points (BL, 18 h, and 24 h) in biological duplicate (n = 30). Samples of the different time points were used for qPCR, 16S-rRNA MiSeq Illumina Sequencing, and SPME GC-MS analyses. After sterile sampling of 5 mL of bioreactor contents, samples were centrifuged at 16,000 × g for 7 min to separate the pellets and the supernatants, which were used for bacterial DNA extraction and SPME-GC-MS analysis, respectively. The pellets were also washed twice in PBS prior DNA extraction. Microbial DNA extraction was conducted just after sampling so as not to reduce *Firmicutes* content. DNA samples and SPME-GC-MS samples were then stored at −80 °C prior analyses. Technical replicas of analyses were conducted in duplicate for SPME GC-MS (n = 60), in triplicate for qPCR (n = 90), and in duplicates for the BL plus pooled duplicates for the end points of fermentation for 16S-rDNA metataxonomy (n = 7).

2.5. Microbiota related analyses

DNA was extracted from the fecal samples (from donors and the pool) and from the MICODE effluates at each time points (BL, 18 h, and 24 h) using the Purelink Microbiome DNA Purification Kit (Invitrogen, Thermo Fisher Scientific, Carlsbad, CA, USA). Nucleic acid purity was tested on BioDrop Spectrophotometer (Biochrom Ltd., Cambridge, UK). Samples from the BL, and the endpoints (EPs) were used for metataxonomy by 16S rRNA MiSeq sequencing (Illumina Inc, San Diego, CA, USA), while samples from the BL and other time points were used for quantitative PCR (qPCR) analyses. Considering metataxonomy, bacterial diversity was obtained by the library preparation and sequencing of the 16S rRNA gene. The following two amplification steps were performed: an initial PCR amplification using 16S locus-specific PCR primers (16S-341F 5′-CCTACGGGNGGCWGCAG-3′ and 16S-805R 5′-GACTACHVGGGTATCTAATCC-3′) and a subsequent amplification integrating relevant flow-cell-binding domains (5′-TCGTCG GCAGCGT-CAGATGTGTATAAGAGACAG-3′ for the forward primer and 5′-GTCTCGTGGGCTCGGAGATGTGTATAAGAGACAG-3′ for the reverse overhang), and lastly unique indices selected among those available Nextera XT Index Kits were combined according to manufacturer's instructions (Illumina Inc, USA). Both input and final libraries were quantified by Qubit 2.0 Fluorometer (Invitrogen, USA). In addition, libraries were quality-tested by Agilent 2100 Bioanalyzer High Sensitivity DNA assay (Agilent technologies, Santa Clara, CA, USA). Libraries were sequenced in a MiSeq (Illumina Inc, USA) in the paired end with 300-bp read length (Marino et al., 2019). Sequencing was conducted by IGA Technology Service Srl (Udine, Italy).

2.6. Sequence data analysis

Reads were de-multiplexed based on Illumina indexing system. Sequences were analyzed using QIIME 2.0 (Bolyen et al., 2019). After filtering based on read quality and length (minimum quality = 25 and minimum length = 200), Operational Taxonomic Units (OTUs) defined by a 97 % of similarity were picked using the Uclust v1.2.22 q method and the representative sequences were submitted to the RDP classifier (Wang et al., 2007) to obtain the taxonomy assignment and the relative abundance of each OTU using the Greengenes 16S rRNA gene database (McDonald et al., 2012) constantly updated by IGA Technology Service Srl (Udine, Italy). Alpha- and beta-diversity analyses were performed using QIIME 2.0.

2.7. Absolute enumeration of bacterial groups by qPCR

Enumeration of bacterial groups was made by qPCR to evidence changes in the microbiota after fermentation (Nissen, Valerii, et al., 2021; Tamargo et al., 2022; Tanner et al., 2014; Tsitko et al., 2019) following previous protocols (Nissen, Valerii, et al., 2021; Nissen et al. 2022, 2023). Specifically, the bacterial groups were selected as

generally accepted indicators of eubiotic or dysbiotic state of colon microbiota; thereafter, their perturbations may be considered closely correlated (directly or inversely) to the prebiotic potential of foods. 16 different bacterial taxa, (Table S1), were assessed by qPCR on a QuantStudio 5 System (Applied Biosystem, Thermo Fisher, USA).

2.8. Volatilome analysis

Volatile organic compound (VOCs) evaluation was carried out on an Agilent 7890A Gas Chromatograph (Agilent Technologies, Santa Clara, CA, USA) coupled to an Agilent Technologies 5975 mass spectrometer operating in the electron impact mode (ionization voltage of 70 eV) equipped with a Chrompack CP-Wax 52 CB capillary column (50 m length, 0.32 mm ID) (Chrompack, Middelburg, The Netherlands). The Solid Phase Micro-Extraction (SPME) GC-MS protocol and the identification of volatile compounds were done according to previous reports, with minor modifications (Casciano et al., 2021; Di Cagno et al., 2011; Nissen, Valerii, et al., 2021). Briefly, 3 mL of vessel content or fecal slurry were placed into 10-mL glass vials and added to 10 μL of the internal standard (4-methyl-2-pentanol) to a final concentration of 4 mg/L. Samples were then equilibrated for 10 min at 45 °C. SPME fiber, coated with carboxen-polydimethylsiloxane (85 μm), was exposed to each sample for 40 min. Preconditioning, absorption, and desorption phases of SPME–GC analysis, and all data-processing procedures were carried out according to previous publications (Casciano et al., 2021; Di Cagno et al., 2011; Nissen, Valerii, et al., 2021). Briefly, before each head space sampling, the fiber was exposed to the GC inlet for 10 min for thermal desorption at 250 °C in a blank sample. The samples were then equilibrated for 10 min at 40 °C. The SPME fiber was exposed to each sample for 40 min, and finally the fiber was inserted into the injection port of the GC for a 10 min sample desorption. The temperature program was: 50 °C for 1 min, then programmed at 1.5 °C/min to 65 °C, and finally at 3.5 °C/min to 220 °C, which was maintained for 25 min. Injector, interface, and ion source temperatures were 250, 250, and 230 °C, respectively. Injections were carried out in split-less mode and helium (3 mL/min) was used as a carrier gas. Identification of molecules was carried out by searching mass spectra in the available databases (NIST 11 MSMS library and the NIST MS Search program 2.0 (NIST, Gaithersburg, MD, USA). Each VOC was relatively quantified in percentage (limit of detection (LOD) = 0.001 mg/kg) (Bonfrate et al., 2020). Besides, in samples prior to *in vitro* colonic fermentation (baseline) the main microbial metabolites related to prebiotic activity were also absolutely quantified in mg/kg (limit of quantitation (LOQ) = 0.03 mg/kg and LOD = 0.01 mg/kg) (Casciano et al., 2021; Di Cagno et al., 2011; Nissen, Valerii, et al., 2021). For these latter compounds, samples at the endpoint (24 h) were compared to the baseline and values were expressed as shifts. All results were expressed as normalized mean values obtained from duplicates in two independent experiments.

2.9. Data processing and statistical analysis

For the microbiota, the dataset for alpha biodiversities indices was generated from the BIOME files of MiSeq analyses, while the beta diversities were process as PCoA (Principal Coordinate of Analysis) employing the EMPeror tool (Vázquez-Baeza et al., 2013) from the QIME 2 pipeline. The dataset for metataxonomy was processed for ANOVA for group comparison (the baseline versus the end point), the significant variables ($p < 0.05$) were selected and the shifts in abundance were calculated as $Log_2(F/C)$ (Hill et al., 2017). The complete R models of ANOVA of family and species level for MiSeq are reported in Tables S3 and S4. Then, *post hoc* Tukey HSD test ($p < 0.05$) was performed on the raw data to define differences among treatments. The microbiota at the endpoint was analyzed as a pool of DNA of the biological replicas for each case, while at the baseline as a pool of the four cases. The Multiple List Comparator tool from https://molbiotools.com/ (last accessed on 28/02/2023) was used to generate pair wise intersection maps and Venn

diagrams. Venn diagrams are supported by Table S5 (exclusive species for each fermentation sample) and Table S6 (shared species among fermentation samples). Log$_2$(F/C) results of family and species levels are presented with Volcano plots, employing VolcanoseR (Goedhart & Luijsterburg, 2020). Volcano plots of family and species levels are supported by descriptive supplemental tables, Tables S7 and S8, respectively. The dataset from qPCR values was processed for MANOVA (Multivariate ANOVA) including two categorical predictors: "time" and "food matrix", then Tukey post hoc test was applied for both categories (Tables S9 and S10). For the volatilome, one-way ANOVA ($p < 0.05$) was used to determine significant VOCs among the dataset, which included 8000 interactions generated between 171 dependent variables (VOCs) and 60 independent variables (2 technical and 2 experimental replicas of 5 different fermentation treatments; AT, AS, CT, CS, and BC, and 3 different time points; BL, T1 = 18 h, and EP = 24 h). The significant VOCs representing the total volatilome were processed by Principal Component Analysis (PCA) to distribute the results on a plane and multivariate ANOVA (MANOVA) to address specific contributes by categorical predictors "time" (Table S11) and "food matrix" (Table S12). Absolute quantification of main principal VOCs at the beginning of colonic fermentation were presented in Table S13. Either the datasets of volatilome and microbiota (metataxonomy and qPCR) were considered for Normality and Homoscedasticity before performing ANOVA/MANOVA models. Normalization of datasets was performed with the mean centering method. Statistics and graphics were also made with Statistica v.8.0 (Tibco, Palo Alto, CA, USA).

3. Results and discussion

3.1. Quality controls for the validation of MICODE protocol

To validate the MICODE experimental approach in the version of fecal batch of the human proximal colon, we chose to monitor and check some parameters as quality controls (QC) related to metabolites and microbes at the end of fermentations, and in comparison, to the baseline. QCs for microbiomics adopted were relative to alpha diversities, that were maintained similar throughout the experimentation. For example, at the EPs, the Chao1 Index, which reflect the microbiota richness, indicated >400 OTUs and the Good's Index, representing the ecological diversity within rare taxa did not change significantly confirming the capacity to simulate a healthy in vivo condition for 24 h and indicating enough support to the growth of rare or less representative species. Also, the presence of *Archea* (*e.g. Methanobrevibacter smithii*), which is extremely sensible to oxygen content (Traore et al., 2019), was retained in the BC vessel from the BL to the EP, indicating that the environmental conditions were strictly maintained. About the volatilome, we evaluated some stool-related compounds, namely urea, 1-propanol, and indole, that were adsorbed at the same retention times spreading across the complete chromatogram and were similarly quantified for each GC/MS analysis. All those indicators confirm the validity of MICODE as *in vitro* model system to study gut microbiota ecology.

3.2. Changes in bacterial alpha and beta diversities

The microbiota diversity indices were analyzed to study the impact of AP breads on colonic microbial population, to assess population's stability during fermentation, and to compare the microbiota of their vessels to that of other bioreactors (Fig. S1). The baseline of value was compared to the endpoints of differently fermented breads. Although not all samples significantly modulated the microbiota, it is undisputable that abundances and richness diminished over time in the *in vitro* simulation of any sample, because no supplementation was considered. For example, at the BL richness was 297.65 ± 133.41 observed OTUs (operational taxonomic units) (Fig. S1A) and abundance was 617.00 ± 273.86 units of Chao1 index (Fig. S1B). After colonic fermentation, both the indices were significantly lower ($p < 0.05$) just for the traditional

baked breads, accounting for 157.61 ± 70.27 and 158.60 ± 70.98 observed OTUs, and 352.14 ± 178.64 and 346.53 ± 175.15 units of Chao1 index, for AT and CT, respectively. No significantly changes for sourdough fermented breads (AS or CS), nor for the BC ($p > 0.05$) were recorded. Evenness and dominance at the BL were 5.37 ± 0.76 units of Shannon index and 0.94 ± 0.02 units of Simpson index (Fig. S1C and S1D) and both were reduced after MICODE fermentation of any sample, but significantly just for AT and CT ($p > 0.05$). In details, AT accounted for 3.18 ± 0.41 units of Shannon index and 0.74 ± 0.04 units of Simpson index, while CT accounted for 3.04 ± 0.37 units of Shannon index and 0.73 ± 0.03 units of Simpson index. These results indicated that sourdough process affected the population diversities less than the traditional one does. The Good's index (Fig. S1E), which estimates the percent of unique species that is represented in a sample, remained unchanged after any fermentation, indicating the effectiveness of the *in vitro* model adopted, that was able to maintain in culture for the whole period of experimentation even rare bacterial taxa. Considering the beta diversity, the Bray Curtis PCoA (Fig. S1F) has drawn larger differences as an effect of time (BL vs EP of fermentations), than as an effect of matrix (AT, AS, CT, CS). Still this outcome is a positive feature for the effectiveness of the *in vitro* model, that indicated different diversities among bioreactors with different samples after their fermentation.

3.3. Changes in taxa abundances at the phylum level

The total sequence reads used in this study were classified into eight phyla and one unassigned (Table S2). In any tested sample, the core microbiota at the BL was represented by four taxa: three with a relative abundance higher than 10 % (*Firmicutes*, *Bacteroidetes*, and *Actinobacteria*) and one lower than 5 % (*Proteobacteria*). Anyhow, just *Firmicutes*, *Bacteroidetes*, and *Proteobacteria* underwent significative changes in comparison to the BL ($p < 0.05$). At this taxonomic level after fermentation the changes were different among the substrates just for *Bacteroidetes*, and *Proteobacteria*, relatively to control samples and the BC.

3.4. Metataxonmy at the family and species level

The dataset of significant OTUs relative to the family and species level is reported in Tables S3 and S4, respectively. The OTUs were filtered up to a cutoff of 0.001 % and among 65 families assigned OTUs in the entire dataset, 33 was the mean number at the BL. After fermentation, just AS was the substrate capable to retain them all, while the other substrates reduced the number of different family taxa.193 OTUs were constructed and assigned to microbial taxa (cutoffs 0.001 %) at the BL. Of these, 171, 146, 152, 150, and 166 were identified at the EPs of fermentation of AS, AT, CS, CT, and BC, respectively (Fig. 1A). At the EP, AS was the substrate that shared most of the taxa found at the BL. Also, from the Intersection Map, the sourdough processed substrates shared more taxa with the BL, than the traditional ones (Fig. 1A). Regarding the exclusive presence of taxa that are relative to each substrate fermentation, (Tables S5 and S6) AS has the highest number, more than the double in respect to AT and CT, and almost four times than CS (Fig. 1B). Among these taxa, AS was characterized by important *Ruminococcus albus*, which is a beneficial commensal, known to be negatively correlated to IBD (Inflammatory Bowel Disease) (Nagao-Kitamoto & Kamada, 2017), but also to harmful *Desulfovibrio*, that is a sulfate reducer culprit of colitis (Rowan et al., 2010). AT at the EP of fermentation was characterized by the exclusive presence of beneficial *Lactobacillus crispatus*, but also to that of *Streptococcus sanguinis*, which is associated to possible infections (Martini et al., 2020). CS was characterized by the exclusive presence of *Streptococcus infantis*, which is a commensal in the oral cavity, but an opportunistic when is transferred to other niches (Zhou et al., 2020). CT was characterized by the exclusive presence of beneficial *Lactobacillus mucosae* (Bagon et al., 2021), but also by that of several opportunistic *Proteobacteria*, such as *Citrobacter* spp.
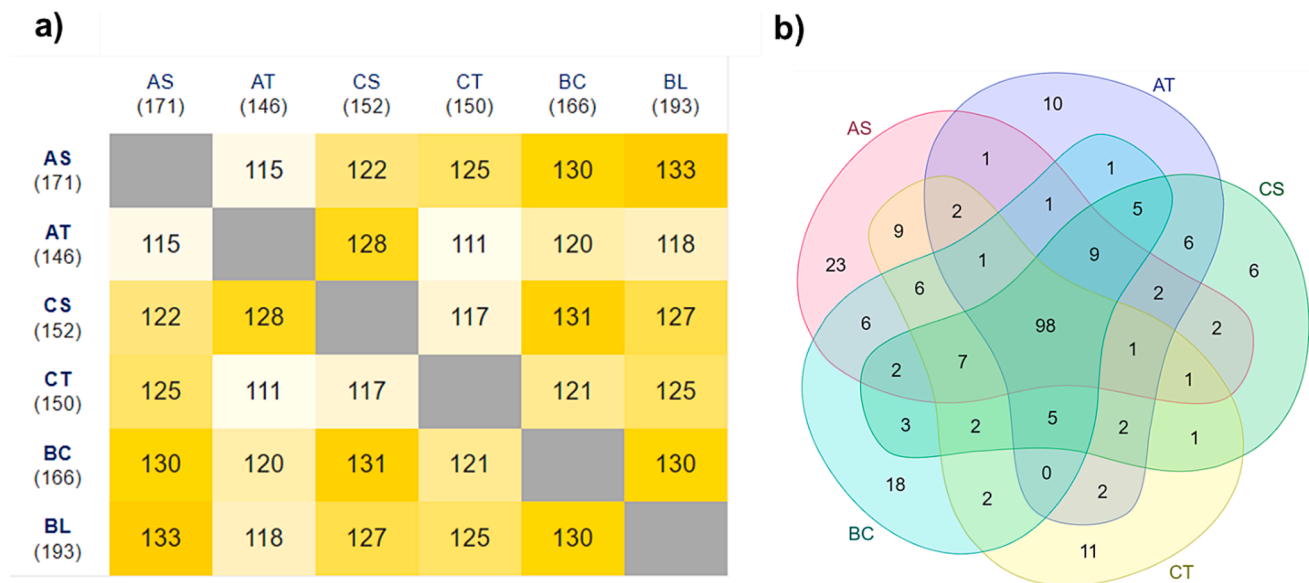
Fig. 1. Pair Wise Intersection Map and Venn Diagrams representing the microbiome lists at species level of human colon microbiota after *in vitro* digestion and fermentation (end points) of algae-enriched gluten-free breads and control gluten-free breads in respect to the baseline. BL = baseline; CS = Control GF sourdough bread; CT = Control GF bread; AS = Algae enriched GF sourdough bread; AT = Algae enriched GF bread; BC = Blank control. Additional information can be found in Tables S5 and S6.

(Liu et al., 2020). Lastly, it is important to note that *Methanobrevibacter smithii* was an exclusive species found in the BC, that is considered as a quality control of our colonic model ecological settings, as this taxon is highly sensible to oxygen (Traore et al., 2019).

*3.5. Changes in taxa abundances at family and species levels*

From the volcano plots for family level (Fig. S2 and Table S7), the results relative to AS (Fig. S2A) substrate fermentation indicated positive outcome as significant changes at family level, like important overrepresentation of beneficial and commensal taxa, as *Bifidobacteriaceae* (>6.67 folds) and *Verrucomicrobiaceae* (>4.35 folds), but also significant underrepresentation of some opportunistic taxa. In contrast, a negative outcome is that of significant underrepresentation of renown families as butyrate producers, such as *Lachnospiraceae* (<2.73 folds) and *Ruminococcaceae* (<4.44 folds).From the volcano plots for species level (Fig. 2 and Table S8), the results relative to AS (Fig. 2A) talked about important overrepresentation of beneficial *Bifidobacterium bifidum* (>5.78 folds) and immunostimulant *Lactobacillus gasseri* (>8.55 folds), bacteriocin producers *Enterococcus durans* (>8.83 folds), and postbiotic producer *Akkermansia muciniphila* (>5.62 folds). Also, still considered as a positive result, the taxa underrepresented in comparison to the BL were those of several opportunistics and metabolic syndrome associated, as *Ruminococcus torques* (<9.42 folds), *R. gnavus* (<5.37 folds), *Dialister invisus* (<2.62 folds), but, as a negative result, also that of commensal *Bacteroides vulgatus* (<3.43 folds) and *Roseburia faecis* (<6.23 folds).

The results relative to AT substrate fermentation indicated positive outcome as significant changes at family level (Fig. S2B), likely important overrepresentation of *Enterobacteriaceae* (>7.09 folds) and *Clostridiaceae* (>4.96 folds), also an underrepresentation of some opportunistic taxa is evidenced, like *Pasteurellaceae* (<4.81 folds), but indicated also negative feature as the reduction of other commensals, as *Ruminococcaceae* (<8.65 folds) and *Lachnospiraceae* (<3.06 folds). At species level (Fig. 2B) there are important overrepresentation of beneficial immunostimulant *L. gasseri* (>6.98 folds) and bacteriocin producers *Enterococcus durans* (>1.85 folds), but also that of opportunistic *Escherichia alberti* (>6.62 folds) and *Clostridium butyricum* (>10.05 folds). As a positive effect, the opportunist *Blautia* was significantly underrepresented (<2.50 folds), but in contrast *A. muciniphila* was

reduced (<2.79 folds).From the recipient results it is evidenced that in general GF breads are not modulating positively the microbiome of not celiac subjects, except when the sourdough process and the enrichment with algae are applied.The results relative to CS substrate fermentation (Fig. S2C) indicated that at family level there are important overrepresentation of *Enterobacteriaceae* (>7.15 folds) and *Lactobacillaceae* (>5.41 folds) and significant underrepresentation of some opportunistic taxa, as *Pastereullaceae* (<3.06 folds). At species level (Fig. 2C) significant overrepresentation of *Lactobacillus gasseri* (>6.67 folds) and *Escherichia alberti* (>6.63 folds) were confirmed, also underrepresentation of several opportunistic *Clostridiales*, but also that of essential *Faecalibacterium* (<6.35 folds). The results relative to CT substrate fermentation (Fig. S2D) indicated that at family level there are important significant overrepresentation of *Enterobacteriaceae* and significant underrepresentation opportunistic clostridia, but also of important *Ruminococcaceae*. At species level (Fig. 2D) significant overrepresentation of *Escherichia alberti* (>5.99 folds) was confirmed, also underrepresentation of *Clostridium butyricum* (<2.18 folds).

3.6. Absolute enumeration of selected bacterial groups from colonic fermentations

Absolute enumeration and the changes in abundance during colonic fermentation of selected bacterial groups were obtained by qPCR, during colonic fermentation (Table 1). Statistical MANOVA models are reported in Tables S9 and S10. *Eubacteria* loads decreased in any colonic fermentation sample with respect to the abundances at the BL. The lowest load recorded after 24 h of colonic fermentation was found after AT fermentation, although no significant difference was observed among the samples at EP ($p < 0.05$). Considering *Firmicutes*, significant reductions were observed at EP for any samples, and the top reduction was signed by AT, although not significant in comparison to other samples at EP ($p < 0.05$).The quantifications of *Bacteroidetes* phylum have shown reductions at any time point by any sample, except for AT mean of reductions ($p < 0.05$). Although no significant difference was observed among the samples at the same time point ($p < 0.05$). Among the beneficial bacterial groups present in the colon, we have quantified the class *Lactobacillales*, the family *Bifidobacteriaceae*, and the *Clostridium* group IV. The shifts related to *Lactobacillales* told that the sourdough
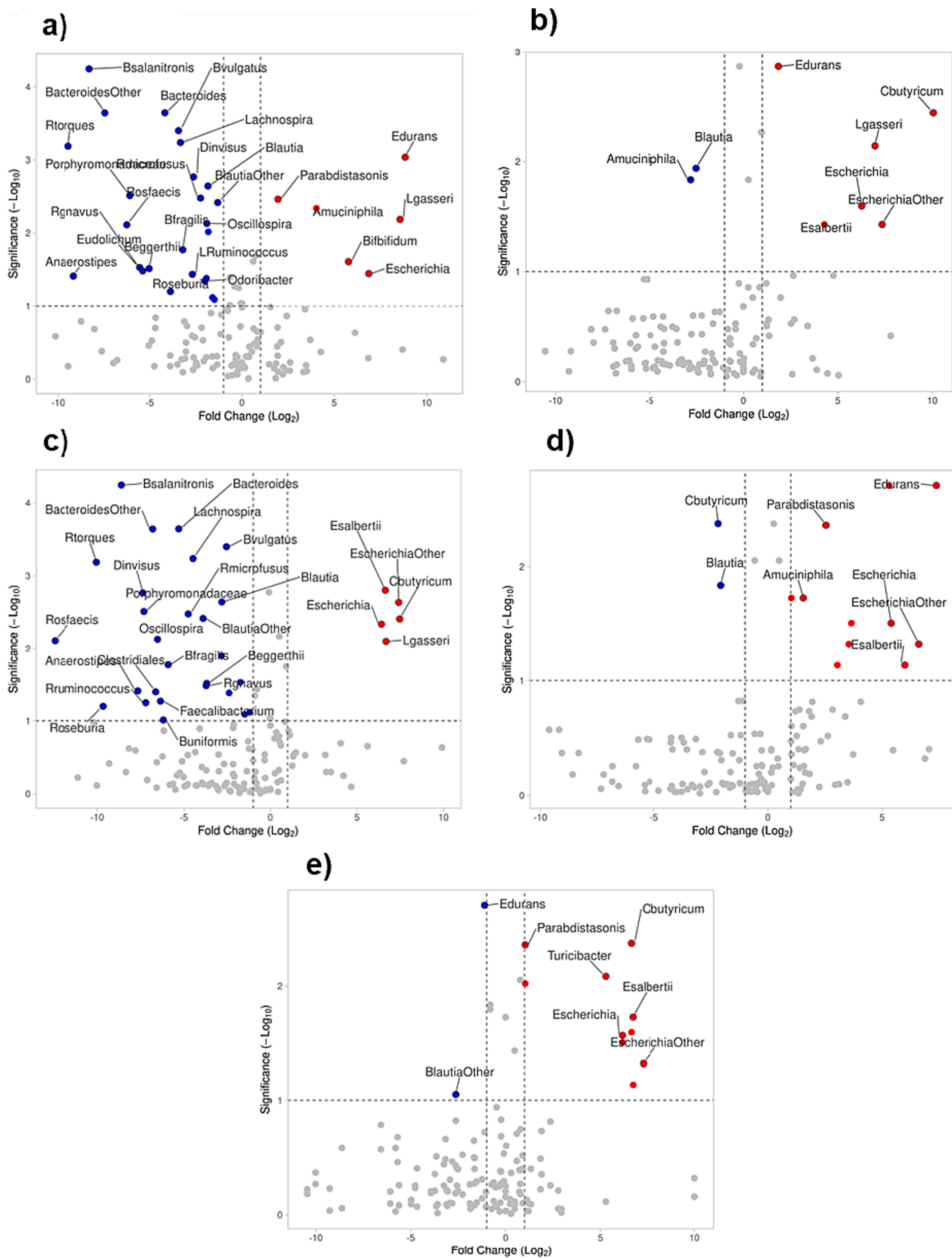
Fig. 2. Volcano plots representing changes of human colon microbiota at species level after *in vitro* digestion and fermentation of AP and control gluten free breads expressed as Log$_2$(F/C) in respect to the baseline. Red dots = overrepresented variables; Blue dots = underrepresented variables; Grey dots = unchanged variables; A) AS = Algae enriched GF sourdough breads; B) AT = Algae enriched GF breads; C) CS = Control GF sourdough breads; D) CT = Control GF breads; E) BC = Blank control. Additional information can be found in Table S8.

Table 1

Quantifications and changes in absolute abundances of core-microbiota taxa measured by qPCR, during colonic fermentation.

qPCR Targets & Samples	Quantifications cells/mL Baseline	ChangesLog$_2$(F/C) T1	EP	MANOVA p (time)
Eubacteria				
CS	5.52E+08 ± 4.38E+07^a	−1.06^b	−1.70^b	0.002636
CT	5.52E+08 ± 4.38E+07^a	−0.73^{ab}	−2.06^b	0.006619
AS	5.52E+08 ± 4.38E+07^a	−0.64^{ab}	−1.61^b	0.033100
AT	5.52E+08 ± 4.38E+07^a	−0.34^a	−2.51^b	0.025183
BC	5.52E+08 ± 4.38E+07^a	−0.63^{ab}	−1.29^b	0.008328
p (food matrix)		0.083719	0.258884	
Firmicutes				
CS	7.05E+07 ± 8.45E+06^a	−1.74^{bB}	−2.35^{bB}	0.038546
CT	7.05E+07 ± 8.45E+06^a	−0.77^{abAB}	−3.14^{bB}	<0.000001
AS	7.05E+07 ± 8.45E+06^a	−1.46^{bB}	−2.67^{bB}	0.015116
AT	7.05E+07 ± 8.45E+06^a	−0.21^{aA}	−3.26^{bB}	<0.000001
BC	7.05E+07 ± 8.45E+06^a	−0.99^{bAB}	−1.14^{bA}	0.001305
p (food matrix)		0.031145	0.000702	
Bacteroidetes				
CS	4.88E+07 ± 6.20E+06^a	−1.30^{bAB}	−1.90^b	0.000599
CT	4.88E+07 ± 6.20E+06^a	−1.22^{bAB}	−2.69^b	0.000317
AS	4.88E+07 ± 6.20E+06^a	−1.42^{bB}	−2.21^b	0.000400
AT	4.88E+07 ± 6.20E+06^a	−1.62^{bB}	−2.22^b	0.034722
BC	4.88E+07 ± 6.20E+06^a	−0.76^{abA}	−1.89^b	0.001404
p (food matrix)		0.026717	0.854455	
Lactobacillales				
CS	2.16E+05 ± 2.82E+04^b	0.61^{abA}	1.17^{aA}	0.003854
CT	2.16E+05 ± 2.82E+04^a	−0.11^{aA}	−2.56^{bB}	0.001229
AS	2.16E+05 ± 2.82E+04^b	1.03^{abA}	1.47^{aA}	0.046415
AT	2.16E+05 ± 2.82E+04^a	−1.22^{bB}	−3.00^{cB}	0.027762
BC	2.16E+05 ± 2.82E+04^a	−1.17^{bB}	−2.48^{bB}	0.048006
p (food matrix)		0.006590	<0.000001	
Bifidobacteriaceae				
CS	2.86E+06 ± 1.23E+05^a	−1.22^{bB}	−2.36^{cB}	0.005974
CT	2.86E+06 ± 1.23E+05^a	−1.36^{bB}	−2.66^{cB}	0.000013
AS	2.86E+06 ± 1.23E+05^b	0.75^{abA}	1.89^{aA}	0.002294
AT	2.86E+06 ± 1.23E+05^b	1.09^{abA}	1.85^{bA}	0.016800
BC	2.86E+06 ± 1.23E+05^a	−0.98^{bB}	−2.32^{cB}	0.000000
p (food matrix)		0.000486	<0.000001	
***Clostridium* group IV**				
CS	2.90E+07 ± 1.19E+06	−0.69^A	−1.21^{AB}	0.359008
CT	2.90E+07 ± 1.19E+06^a	−2.24^{bB}	−3.70^{bC}	0.023000
AS	2.90E+07 ± 1.19E+06	−0.30^A	−0.55^A	0.211192
AT	2.90E+07 ± 1.19E+06	−0.70^A	−1.68^B	0.772915
BC	2.90E+07 ± 1.19E+06^a	−3.83^{bB}	−4.53^{bC}	0.040232

Table 1 (*continued*)

qPCR Targets & Samples	Quantifications cells/mL Baseline	ChangesLog$_2$(F/C) T1	EP	MANOVA p (time)
p (food matrix)		<0.000001	<0.000001	
Enterobacteriaceae				
CS	1.29E+06 ± 5.54E+06^b	0.37^{bB}	1.70^{aB}	0.011160
CT	1.29E+06 ± 5.54E+06^c	2.41^{bA}	4.35^{aA}	0.004343
AS	1.29E+06 ± 5.54E+06^b	1.61^{aA}	1.81^{aB}	0.025476
AT	1.29E+06 ± 5.54E+06^b	2.27^{aA}	4.03^{aA}	0.001924
BC	1.29E+06 ± 5.54E+06^b	0.33^{bB}	2.01^{aB}	0.047383
p (food matrix)		0.044738	0.034866	
ATOP group				
CS	1.54E+05 ± 3.09E+04^b	1.29^{aB}	1.46^{aB}	0.000003
CT	1.54E+05 ± 3.09E+04^b	3.95^{aA}	4.85^{aA}	<0.000001
AS	1.54E+05 ± 3.09E+04	−0.23^C	−0.86^C	0.084866
AT	1.54E+05 ± 3.09E+04	0.21^{BC}	0.32^{BC}	0.130894
BC	1.54E+05 ± 3.09E+04	0.37^{BC}	0.78^B	0.084486
p (food matrix)		<0.000001	0.000458	
***Clostridium* group I**				
CS	1.16E+05 ± 2.45E+04^b	0.42^{abAB}	1.25^{aB}	<0.000001
CT	1.16E+05 ± 2.45E+04^a	1.12^{bA}	3.86^{aA}	0.000143
AS	1.16E+05 ± 2.45E+04	−0.01^B	−0.72^C	0.462310
AT	1.16E+05 ± 2.45E+04	0.84^{AB}	1.25^B	0.076147
BC	1.16E+05 ± 2.45E+04^b	1.52^{aA}	1.74^{aB}	0.023171
p (food matrix)		0.017931	0.044531	
Escherichia coli				
CS	6.32E+05 ± 3.71E+04^b	2.58^{aA}	3.63^{aA}	0.000016
CT	6.32E+05 ± 3.71E+04^c	1.67^{bB}	4.84^{aA}	0.003585
AS	6.32E+05 ± 3.71E+04^b	1.48^{aB}	2.06^{aB}	<0.000001
AT	6.32E+05 ± 3.71E+04^b	2.60^{aA}	3.36^{aA}	0.008608
BC	6.32E+05 ± 3.71E+04^c	1.42^{bB}	3.23^{aA}	<0.000001
p (food matrix)		0.025882	0.000001	
***Desulfovibrio* spp.**				
CS	2.66E+03 ± 4.32E+02^b	1.56^a	1.64^{aB}	0.045958
CT	2.66E+03 ± 4.32E+02^b	1.38^b	3.45^{aA}	0.045481
AS	2.66E+03 ± 4.32E+02^a	−0.70^{ab}	−0.93^{bC}	0.019299
AT	2.66E+03 ± 4.32E+02^b	0.67^b	3.40^{aA}	0.010731
BC	2.66E+03 ± 4.32E+02	0.25	0.57^{BC}	0.482995
p (food matrix)		0.182351	0.007095	

[A,B,C] Different capital letters indicate significance difference within a column; [a,b,c] Different lower-case letters indicate significance difference within a row according to MANOVA model followed by Tukey's HSD test ($p < 0.05$). MANOVA p value stands for italicized numbers relative to time effect on rows and to matrix effect on columns. BL = Baseline; T1 = 18 h of fermentation; EP = 24 h of fermentation. CS = Control GF sourdough bread; CT = Control GF bread; AS = Algae enriched GF sourdough bread; AT = Algae enriched GF bread; BC = Blank control. Additional information can be found in Tables S8 and S9.

samples AS and CS once fermented in the colon bring to over-representation, while the control sample AT and CT bring to underrepresentations. The shifts related to *Bifidobacteriaceae* had a different trend, as both the algae fortified sample AS and AT were able to foster this family, while the standard breads CS and CT were not. Considering the *Clostridium* group IV, any sample at any time point recorded underrepresentations, with the top reduction hit by CT and the minimum one by AS. Among the opportunistic bacterial groups present in the colon, we have selected and quantified five taxa, namely: the family *Enterobacteriaceae*, the *Atopobium - Collinsella - Eggerthella* (ATOP) group, the *Clostridium* group I, the genus *Desulfovibrio* spp., and the species *Escherichia coli*. The shifts recorded by *Enterobacteriaceae,* and *E. coli* were of the same trend, indicating overrepresentation for any sample at any time point. The top increases at the EP were that relative to the controls CT and AT, while the minimum increases were relative to AS fermentation. For example, CT increases *Enterobacteriaceae* almost 6 times more than AS. Considering *E. coli*, still CT was the fermentation that led to the top increase and AS to the minimum one, with CT values accounting as almost 7 times more than AS. The shifts relative to the ATOP group at EP recorded top overrepresentations for CT and underrepresentation for AS. The shifts recorded by *Clostridium* group I indicated a top overrepresentation whit CT, and a top underrepresentation scored by AS. Lastly, the shifts recorded by *Desulfovibrio* spp. indicated a similar ($p > 0.05$) overrepresentation of CT and AT, and underrepresentation of AS.Generally, these results suggested that despite a general reduction in the absolute abundance of total bacteria, reported also at the phylum level for *Firmicutes* and *Bacteroidetes*, the GF breads obtained by control process (AT and CT), were not able to foster any beneficial taxa, except for AT and *Bifidobacteriaceae* and did trigger increases for any opportunistic taxa examined. In contrast, the breads obtained with sourdough process, notably AS, once fermented by the colon generated increases on beneficial taxa and minor increase on opportunistic taxa, with AS able even to reduce the content of ATOP group, *Clostridium* group I, and *Desulfovibrio* spp., although not significantly ($p > 0.05$).

3.7. Volatilome analysis through SPME GC/MS

Through SPME GC-MS, among 30 duplicated cases (n = 60), 171 molecules were identified with >80 % of similarity with NIST 11 MS library and the NIST MS Search program 2.0 (NIST, Gaithersburg, MD,

USA). Syntax of molecules name is that of the NIST 11 MS Library, where official names are reported with the first initial in capital letter, while synonyms are reported with first initial in lower case, for example: 1H-Indole, 3-methyl and skatole. From the Pair Wise intersection Map (Fig. 3A) on average, 125 were relatively quantified at the BL, while 108, 101, 93, and 95 were quantified during the 24 h of experiments at different timepoints for AS, AT, CS, and CT, respectively Also 74 VOCs were averagely found during fermentation in the BC. Regarding the Venn Diagram (Fig. 3B) is interesting to mention that the highest number of exclusive VOCs were found in AS area (9), AT area (7) and at their intersection (18). Some of the exclusive VOCs found in AS were Caryophillene, m-Cymene-5-*tert*-butyl, and Beta-Alanina, while some of those found in CS were 3-Tridecene (Z) and Furan, 2-methoxy.
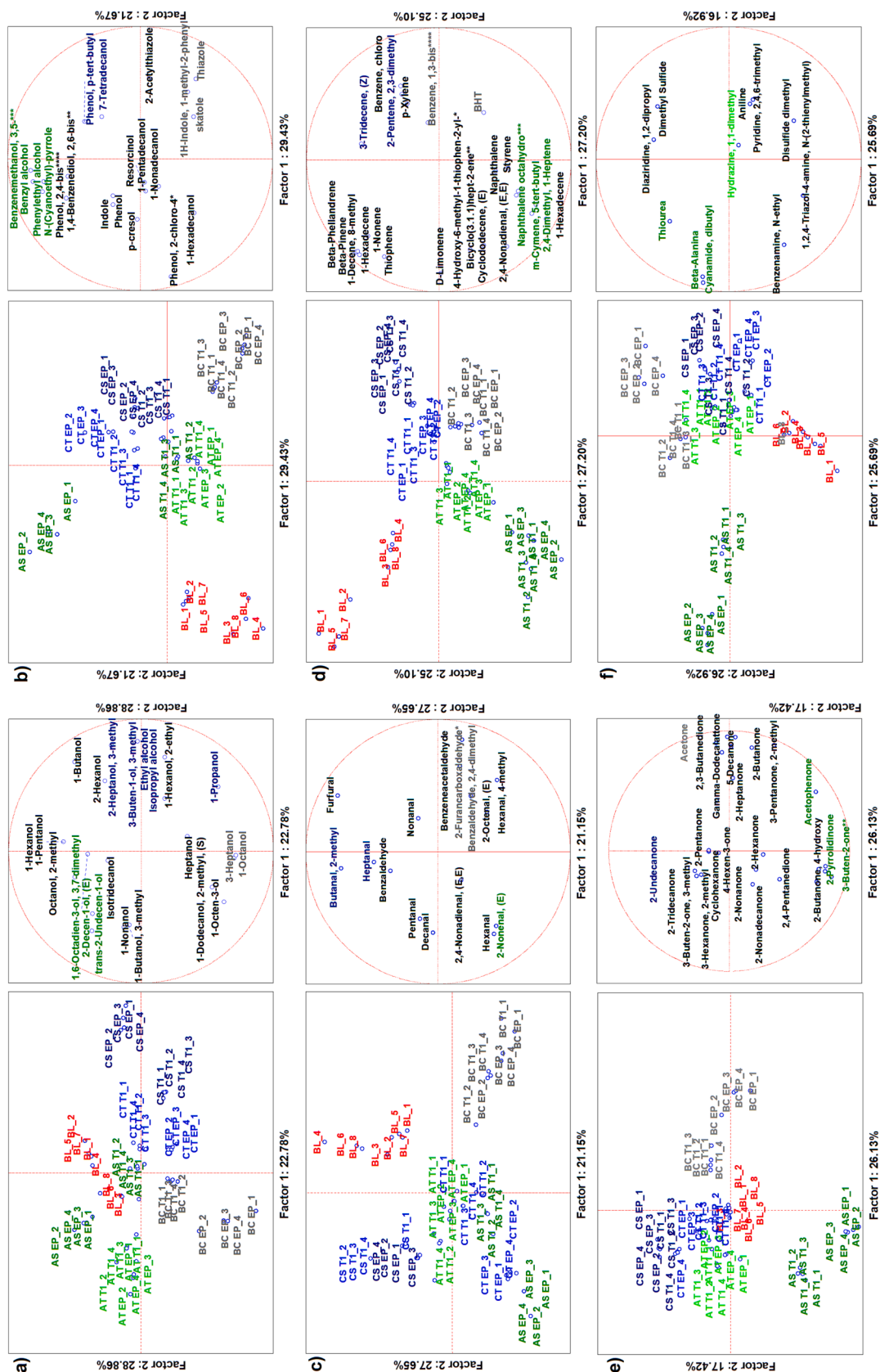
Principal Component Analysis (PCA) (Fig. 4) and targeted MANOVA ($p < 0.01$) (Tables S11 and S12) were achieved to address the specific contributes to VOCs production by the independent variables. Supernormalization of the dataset was essential to unveil the effect of those compounds that are less volatile than others and could be underrepresented, as well as to avoid comparing one chemical class to another. In these datasets T1 cases are also considered.

A PCA of 22 statistically significant low molecular alcohols distributed cases on the plot, separating fermentation with algae breads to that of control breads, and the BC from each other and from the baseline (Fig. 4A). By MANOVA the main descriptors of algae enriched breads were 1,6-Octadien-3-ol, 3,7-dimethyl, 2-Decen-1-ol, (E), and *trans*-2-Undecen-1-ol, chiefly produced by the sourdough process at the EP. In contrast descriptors of control breads were 2-Heptanol, 3-methyl, Ethyl alcohol, Isopropyl alcohol, and 1-Propanol, mainly produced by the sourdough process at the EP of fermentation. Thus, alcohols derived from the matrix are including Geraniol and olefins as descriptors of AS, while alcohols derived mainly from colonic fermentation are descriptors of CS. Thus, the discrimination of low molecular alcohols was dependent on the food matrix used, more than on the process of fermentation. Geraniol is known to own an antioxidant nature and it is originally found in spirulina enriched breads (Casciano et al., 2021). Geraniol as a dietary monoterpene is a potent bioactive, that is able to ameliorate intestinal dysbiosis, also acting as a prebiotic towards the growth of some beneficial microbes, as members of *Clostridium* group IV (Rizzello et al., 2018). From our data the presence of Geraniol in algae enriched breads could partially explain the overrepresentation of *Clostridium* group IV
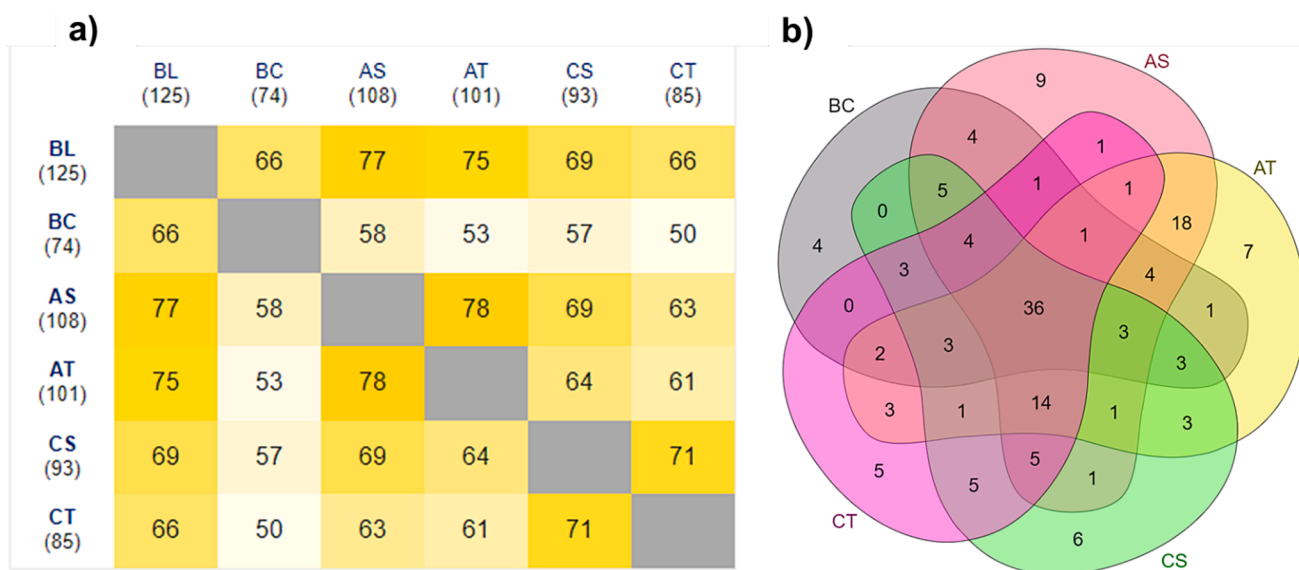
Fig. 3. Pair Wise Intersection Map and Venn Diagrams representing the volatilome list of VOCs of human colon microbiota after *in vitro* digestion and fermentation (end points) of algae-enriched gluten-free breads and control gluten-free breads in respect to the baseline. BL = baseline; CS = Control GF sourdough bread; CT = Control GF bread; AS = Algae enriched GF sourdough bread; AT = Algae enriched GF bread; BC = Blank control.

Fig. 4. Principal Component analysis and Multivariate Analysis of Variance of volatile organic compounds (VOCs) production by colonic fermentation of different samples. a) Low molecular alcohols VOCs; b) high molecular alcohols VOCs; c) aldehydes VOCs; d) alkenes; e) ketones; f) amines and sulphurated VOCs. Left side diagrams are for cases; Right side diagrams are for variables. Additional information on the % of contribution of VOCs production can be found in Tables S10 and S11. BL = baseline; T1 = intermediate time point; EP = endpoint; CS = Control GF sourdough bread; CT = Control GF bread; AS = Algae enriched GF sourdough bread; AT = Algae enriched GF bread; BC = Blank control.

once these samples were fermented by colon microbiota.

A PCA of 20 statistically significant high molecular alcohols distributed cases on the plot, separating fermentation with AS, AT, control breads, and the BC from each other and from the BL (Fig. 4B). From our results, the group of cases of AS was set as the most distant to BL of fermentation. The main descriptors of fermentation with AS were mainly complex alcohols ($p < 0.01$), such as N-(Cyanoethyl)-pyrrole, Benzyl alcohol, and Phenylethyl alcohol mainly produced at the EP ($p < 0.01$) while those for control breads were Phenol, p-*tert*-butyl and 7-Tetradecanol, mainly produced by the sourdough process either at T1 or EP ($p < 0.01$). The main descriptor of alcohol production from BC samples were instead skatole and Thiazole largely produced at the EP ($p > 0.01$). Thus, AS had the exclusive sign of bioactive such as N-(Cyanoethyl)-pyrrole, that is a catabolic block of phycocyanin, the top antioxidant compound present in spirulina (Casciano et al., 2021). Differently, long chain fatty alcohols derived mainly from colonic fermentation, but also food contaminants are descriptors of CS. Even for this class of molecules, the discrimination found by multivariate analysis was dependent on the food matrix used, more than on the process of fermentation. Notwithstanding, the signature of N-(Cyanoethyl)-pyrrole in AS samples could be due to the catabolic activity of sourdough lactobacilli, already degrading phycocyanin during the leavening process, and the action of intestinal lactobacilli, that were indeed overrepresented just after colonic fermentation of AS. A PCA of 15 statistically significant aldehydes distributed cases on the plot, separating fermentation with AS and CS distant to each other and distant from the BL and the BC (Fig. 4C). The main descriptor of fermentation with AS was 2-Nonenal, (E), mainly produced at the EP ($p < 0.01$). The main descriptors of fermentation with CS were Butanl-2-methyl and Heptanal ($p < 0.01$), while those of the BC were Benzaldehyde, 2,4-dimethyl and 2-Furancarboxaldheyde either produced at T1 and EP ($p < 0.01$). Aldehydes are a result of microbial fermentation and lipid oxidation. Certain aldehydes are health-promoters, like indole-3-aldehyde that regulates host physiology and immunity (Zelante et al., 2021), while most are detrimental, being cytotoxic at a low threshold, such as Benzeneacetaldheyde (Zhang et al., 2020). In our dataset, 2-Nonenal was a descriptor of colonic fermentation of AS. This feature could be due to the high lipid content of algae, as this VOC is known as a major oxidation product of fish oils (Zhang et al., 2020). Its presence could be toxic for the host, thus must be monitored during leavening. A PCA of 23 statistically significant alkenes VOCs distributed cases on the plot, separating the substrates from each other and from the baseline (Fig. 4D). The main descriptor of fermentation with AS were Naphthalene octahydro, 2,4-dimethyl-heptene, and m-Cymene, 5-*tert*-butyl, and Caryophillene mainly produced at the EP of fermentation ($p < 0.01$). While the main descriptors of CS were 3-Tridecene, (Z) and 3-Pentene, 2,3-dimethyl, either produced at T1 or EP. Caryophillene and m-Cymene, 5-*tert*-butyl are potent health-related terpenes (Nissen et al., 2020, 2023) and the features observed indicate that the descriptors of AS were not subject to fermentation and thus their bioactivity was preserved from the food matrix. Thus, while bioactives and antioxidant terpenes are descriptors of colonic fermentation of AS, olefins and food additives are retained in higher portion after digestion and colonic fermentation of controls as are descriptors of CS. A PCA of 22 statistically significant ketones VOCs distributed cases on the plot, separating the substrates from each other and from the baseline (Fig. 4E). The main descriptors of fermentation with AS were Acetophenone, 2-Pyrrolidinone, and 3-Buten-2-one, 4-methyl. Acetophenone is a desirable ketone produced during colonic fermentation thanks to its antimicrobial activity against different Gram-negative bacteria and its *N*-substitute derivates are good inhibitors of the α-glicosidase enzyme, representing a promising therapeutic approach in diabetes (Taslimi et al., 2020). The main descriptor of fermentations with CS was 2-Undecanone, while that of BC was Acetone, both produced mainly at EP. During colonic fermentation, many ketones are produced. Considering their bioactivity, some are desirable, such as the ketones bodies, ad alternative fuel source for the brain (Gross et al., 2019); others, such as

Acetone, are unwanted because they could be toxic for the host (Young et al., 2020). A PCA of 23 statistically significant amines VOCs distributed cases on the plot, separating the substrates from each other and from the baseline (Fig. 4F). The main descriptor of fermentation of AT was Hydrazine, 1,1-dimethyl, while those of AS were Thiourea, Beta-Alanine, and Cyanamide, dibutyl. Beta-Alanine, an isomer of alanine, is a non-protein amino acid sourced from intestinal bacteria by the reaction between propionic acids and ammonia (Powles et al., 2022).

3.8. Quantification of principal microbial metabolites in form of volatile organic compounds

Production of volatile organic acids, either short chain fatty acids and medium chain fatty acids is a fundamental process of a proper colon metabolism after intake of a food and also a potent indicator of the colon microbiota eubiosis. Additionally, an augmented quantity of these compounds at the end of fermentation is a potent indicator of food functionality. These compounds, namely acetic, propanoic, butanoic, pentanoic, and hexanoic acids were produced in respect to the baseline (Table S13) by any samples, except for the BC, that did not significantly produce any (Fig. 5A).

In details, AS was able to increase significantly the quantity of all compounds, with top production in the dataset of acetic, butanoic, and hexanoic acids. AS fermentation was the best performer among the GF breads, and in respect to the baseline produced roughly: i) six times higher acetic acid than any other samples; ii) eight times higher butanoic acid, that doubled the production of the second runners CS and CT; iii) eight times higher hexanoic acids than any other samples, but four times higher than CS. Production of these beneficial compounds by fermentation of algae has been documented previously, up to that algae are now used as a platform to produce high amount of C2–C6 volatile fatty acids (Magdalena and González-Fernández, 2019). Dual production of either short or medium chain fatty acids is a trustworthy indicator of a consortium activity of beneficial bacteria in metabolizing a desirable substrate. In fact, as acetic and butanoic acids are derived in the colon from degradation of insoluble fibers by beneficial clostridia lactobacilli and bifidobacteria, the hexanoic production is derived from the elongation of shorter chain lactic acid (Fujita et al., 2007), chiefly by lactobacilli. In line with the literature, after AS fermentation, these taxa were all surged in abundance. From the results relative to detrimental compounds (Fig. 5B), in respect to the BL of colonic fermentation (Table S13), the significant changes evidenced by the breads fermentation are referred just to sourdough samples AS and to CS. In details: i) AS during fermentation increased about three times more the production of Phenol; ii) AS increased about four times more the amount of p-cresol and iii) AS produced about five times more Phenol than CS, that was the sole sample fermentation able to reduce it. Eventually, the higher abundance of phenols after AS fermentation could be due to the higher presence of phenolics derived from algae enrichment. In particular, spirulina is rich in phenolic compounds, like chlorophylls, carotenoids, and phycocyanin (Bortolini et al., 2022). The partial degradation of these compounds by specialized colonic microbial taxa, as lactobacilli, clostridia, bifidobacteria is reported and well described (Selma et al., 2009) and could be the responsible in the surge of phenolic monomers. When a microbiota is not in eubiosis, the indole quantity produced by colonic fermentation of proteins and in particular of tryptophan and tyrosine accumulate in the colon and get transformed by opportunistic microbes, likely *E. coli* and *Clostridium* group I, in more detrimental compounds, such as skatole (Nissen et al., 2023), which affect the mucosa and causes the production of inflammatory cytokines (Roager & Licht, 2018). Other known detrimental compounds that are hallmarks of *Proteobacteria* fermentation of proteins, chiefly Phenol and p-cresol, when accumulate in the colon triggers specific insults, such as the impairment of epithelial barrier function (Wang et al., 2020). Additionally, p-cresol and Indole would be transformed into p-cresyl sulphate and indoxyl sulphate, which after conjugation, accumulates in
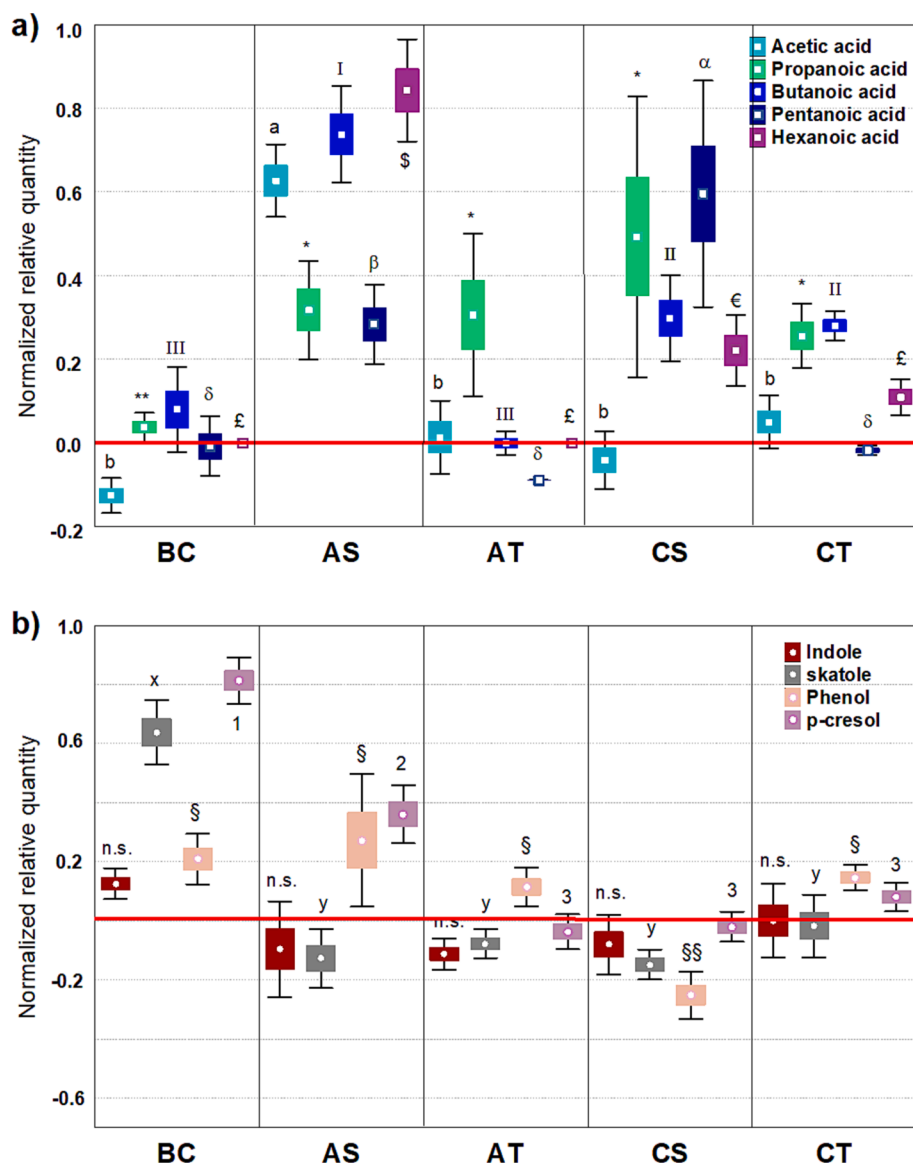
Fig. 5. Principal Component analysis and Multivariate Analysis of Variance of volatile organic compounds (VOCs) production by colonic. a) Beneficial VOCs; b) Detrimental VOCs. Each plot is made with the raw data obtained from each time point and replica. Each value was obtained from technical duplicate from two independent experiments (n = 4). Marker = mean; box = mean ± S.D.; whiskers = Confidence Interval 0.95. Cases with different letters or numbers or symbols among a single independent variable are significantly different, according to ANOVA model followed by Tukey's HSD test ($p < 0.05$). ns = not significant ($p > 0.05$). Red line = baseline; CS = Control GF sourdough bread; CT = Control GF bread; AS = Algae enriched GF sourdough bread; AT = Algae enriched GF bread; BC = Blank control.

the liver leading to complications and pathologies such as chronic kidney diseases and cardiovascular diseases (Arcidiacono et al., 2022).

4. Conclusion

Our principal hypothesis was that transforming biotechnologically the GF breads with algae enrichment and sourdough process we could ameliorate the negative impact of GF breads on host colon ecology of not-celiac consumers. In fact, the impact of control GF breads on the colon ecology of not-celiac representative microbiota is inducer of opportunistic overgrowth, raising the numbers of *Enterobacteriaceae*. Otherwise, the response to our hypothesis was given by mitigation of this negative effect with biotechnological transformation. In fact, when a sourdough fermentation is applied to the breads, it results in a positive modulation of the colon microbiota in respect to the beneficial taxa, even if the effects on their metabolites are more complex. Based on this scenario, our results indicate that the combination of sourdough

fermentation and algae breads is able to exert a prebiotic effect, fostering some beneficials gut populations, limiting some opportunistic ones, producing more short chain fatty acids, and also permit an higher retention of bioactive compounds.

The next step will be identifying statistical correlations between microbiomics and metabolomics data sets also by means of machine learning approach, using for example a recently developed K-cliques multiomic framework applied to food research (Mengucci et al., 2022). Also, a comprehensive characterization of the phenolic profile of the algae-enriched breads, prior, during, and after gastro-intestinal digestion, to elucidate the degradation pathway of phenols and the microbiota involvement needs further investigations. As future perspectives to confirm and extend these results investigations with an *in vitro* gut celiac model and a long-term approach are suggested. Results from the *in vitro* model would serve as a solid foundation for clinical applications and nutritional intervention trial, including any side effects of restricted diets to common consumers, and also serve as a tool to reduce the animal

testing. A harmonization of different *in vitro* models together with the creation of multi-omics shared data sets would support clinical studies by a deep knowledge of gut-food interactions. The use of MICODE, a robust and versatile *in vitro* gut model, along multivariate statistic visibly demonstrated a suitable approach to describe the effects generated by GF foods on healthy individuals. Such *in vitro* approach could be included in a pipeline of experiments where a reduced number of animals for testing is employed, according to the Directive 2010/63/EU and the Regulation (EU) 2019/1010. To fully understand the effect of GF breads on human health of not-celiac subjects a diet intervention study is imperative, and the results presented are target-effective and should have robustness for pre-clinical applications.

Institutional review board statement

The study was conducted according to the guidelines of the ethics procedures required at the University of Bologna.

Informed consent statement

Informed consent was obtained from all subjects involved in the study.

Funding

CRediT authorship contribution statement

Lorenzo Nissen: Supervision, Visualization, Writing – review & editing, Writing – original draft, Data curation, Investigation, Formal analysis, Validation, Methodology, Conceptualization. **Flavia Casciano:** Writing – review & editing, Data curation, Formal analysis, Investigation. **Elena Chiarello:** Writing – review & editing, Investigation, Formal analysis. **Mattia Di Nunzio:** Supervision, Writing – review & editing, Investigation, Formal analysis, Validation, Methodology, Conceptualization. **Alessandra Bordoni:** Funding acquisition, Project administration, Supervision, Writing – review & editing, Resources, Investigation, Validation, Methodology, Conceptualization. **Andrea Gianotti:** Funding acquisition, Project administration, Supervision, Visualization, Writing – original draft, Data curation, Resources, Investigation, Validation, Methodology, Conceptualization.

Declaration of Competing Interest

The authors declare that they have no known competing financial interests or personal relationships that could have appeared to influence the work reported in this paper.

Data availability

Data will be made available on request.

Appendix A. Supplementary material

Fig. S1. Ecological diversities representing the baseline and the end points of colonic fermentation of human colon microbiota. **Fig. S2.** Volcano plots representing changes of human colon microbiota at family level. **Table S1.** PCR Primers and condition of qPCR reactions. **Table S2.** Metataxonomy of Abundances and Changes of Human Colon Microbiota. **Table S3.** Test of SS whole model vs SS residuals of ANOVA at family level. **Table S4.** Test of SS whole model vs SS residuals of ANOVA at species level. **Table S5.** Venn Diagram exclusive species for each fermentation sample. **Table S6.** Venn Diagram shared species among fermentation samples. **Table S7.** VolcaNoseR - Exploring volcano plots

relative to microbiota changes at the end points after in vitro digestion and fermentation at family level. **Table S8.** VolcaNoseR - Exploring volcano plots relative to microbiota changes at the end points after in vitro digestion and fermentation at species level. **Table S9.** R Models from MANOVA analyses categorized for the "time effect" of qPCR data. **Table S10.** R Models from MANOVA analyses categorized for the "food matrix effect" of qPCR data. **Table S11.** MANOVA categorized for the "time effect". % of contribution of Volatile Organic Compounds production. **Table S12.** MANOVA categorized for the "food matrix effect". % of contribution of Volatile Organic Compounds production. **Table S13.** Quantification of the main volatile microbial metabolites at the beginning of colonic fermentations (baseline values). Supplementary data to this article can be found online at https://doi.org/10.1016/j.foodchem.2023.137633.

References

Aguiar, E. V., Santos, F. G., Krupa-Kozak, U., & Capriles, V. D. (2021). Nutritional facts regarding commercially available gluten-free bread worldwide: Recent advances and future challenges. *Critical Reviews in Food Science and Nutrition*, 1–13. https://doi.org/10.1080/10408398.2021.1952403

Arcidiacono, T., Magni, G., Macrina, L., Sirtori, M., Belloni, C., Premaschi, S., … Vezzoli, G. (2022). Serum irisin may predict cardiovascular events in elderly patients with chronic kidney disease stage 3-5. *Journal of Renal Nutrition, 32*(3), 282–291.

Arnal, M. E., Denis, S., Uriot, O., Lambert, C., Holowacz, S., Paul, F., Kuylle, S., Pereira, B., Alric, M., & Blanquet-Diot, S. (2021). Impact of oral galenic formulations of *Lactobacillus salivarius* on probiotic survival and interactions with microbiota in human in vitro gut models. *Beneficial Microbes, 12*(4), 75–90. https://doi.org/10.3920/BM2020.0187

Bagon, B. B., Oh, J. K., Valeriano, V. D. V., Pajarillo, E. A. B., & Kang, D. K. (2021). Exploring the bile stress response of *Lactobacillus mucosae* LM1 through exoproteome analysis. *Molecules, 26*(18), Article 5695. https://doi.org/10.3390/molecules26185695

Bolyen, E., Rideout, J. R., Dillon, M. R., Bokulich, N. A., Abnet, C. C., Al-Ghalith, G. A., … Caporaso, J. G. (2019). Reproducible, interactive, scalable and extensible microbiome data science using QIIME 2. *Nature Biotechnology, 37*(8), 852–857. https://doi.org/10.1038/s41587-019-0209-9

Bonfrate, L., Di Palo, D. M., Celano, G., Albert, A., Vitellio, P., De Angelis, M., Gobbetti, M., & Portincasa, P. (2020). Effects of *Bifidobacterium longum* BB536 and *Lactobacillus rhamnosus* HN001 in IBS patients. *European Journal of Clinical Investigations, 50*(3), e13201.

Bortolini, D. G., Maciel, G. M., Fernandes, I. D. A. A., Pedro, A. C., Rubio, F. T. V., Branco, I. G., & Haminiuk, C. W. I. (2022). Functional properties of bioactive compounds from *Spirulina* spp.: Current status and future trends. *Food Chemistry: Molecular Sciences*, Article 100134.

Casciano, F., Nissen, L., & Gianotti, A. (2021). Effect of formulations and fermentation processes on volatile organic compounds and prebiotic potential of gluten-free bread fortified by spirulina (*Arthrospira platensis*). *Food and Function, 12*(20), 10226–10238. https://doi.org/10.1039/d1fo01239h

Connolly, M. L., Tuohy, K. M., & Lovegrove, J. A. (2012). Wholegrain oat-based cereals have prebiotic potential and low glycaemic index. *British Journal of Nutrition, 108*(12), 2198–2206. https://doi.org/10.1017/S0007114512000281

Di Cagno, R., De Angelis, M., De Pasquale, I., Ndagijimana, M., Vernocchi, P., Ricciuti, P., … Francavilla, R. (2011). Duodenal and faecal microbiota of celiac children: Molecular, phenotype and metabolome characterization. *BMC Microbiology, 11*, Article 219. https://doi.org/10.1186/1471-2180-11-219

Fradinho, P., Niccolai, A., Soares, R., Rodolfi, L., Biondi, N., Tredici, M. R., Sousa, I., & Raymundo, A. (2020). Effect of *Arthrospira platensis* (spirulina) incorporation on the rheological and bioactive properties of gluten-free fresh pasta. *Algal Research, 45*, Article 101743.

Fujita, Y., Matsuoka, H., & Hirooka, K. (2007). Regulation of fatty acid metabolism in bacteria. *Molecular Microbiology, 66*(4), 829–839. https://doi.org/10.1111/j.1365-2958.2007.05947.x

Goedhart, J., & Luijsterburg, M. S. (2020). VolcaNoseR is a web app for creating, exploring, labeling and sharing volcano plots. *Scientific Reports, 10*(1), Article 20560.

Gross, E. C., Klement, R. J., Schoenen, J., D'Agostino, D. P., & Fischer, D. (2019). Potential protective mechanisms of ketone bodies in migraine prevention. *Nutrients, 11*(4), Article 811. https://doi.org/10.3390/nu11040811

Hill, C. J., Lynch, D. B., Murphy, K., Ulaszewska, M., Jeffery, I. B., O'Shea, C. A., … Stanton, C. (2017). Evolution of gut microbiota composition from birth to 24 weeks in the INFANTMET cohort. *Microbiome, 5*, 4. https://doi.org/10.1186/s40168-016-0213-y

Lafarga, T., Fernández-Sevilla, J. M., González-López, C., & Acién-Fernández, F. G. (2020). Spirulina for the food and functional food industries. *Food Research International, 137*, Article 109356.

Liu, L., Qin, L., Hao, S., Lan, R., Xu, B., Guo, Y., … Zhao, C. (2020). Lineage, antimicrobial resistance and virulence of *Citrobacter* spp. *Pathogens, 9*(3), Article 195. https://doi.org/10.3390/pathogens9030195

Magdalena, J. A., & González-Fernández, C. (2019). Microalgae biomass as a potential feedstock for the carboxylate platform. *Molecules, 24*(23), Article 4404. https://doi.org/10.3390/molecules24234404

Marino, M., Dubsky de Wittenau, G., Saccà, E., Cattonaro, F., Spadotto, A., Innocente, N., … Marroni, F. (2019). Metagenomic profiles of different types of Italian high-moisture Mozzarella cheese. *Food Microbiology, 79*, 123–131. https://doi.org/10.1016/j.fm.2018.12.007

Martini, A. M., Moricz, B. S., Ripperger, A. K., Tran, P. M., Sharp, M. E., Forsythe, A. N., … Jones, B. D. (2020). Association of novel *Streptococcus sanguinis* virulence factors with pathogenesis in a native valve infective endocarditis model. *Frontiers in Microbiology, 11*, Article 10. https://doi.org/10.3389/fmicb.2020.00010

McDonald, D., Price, M. N., Goodrich, J., Nawrocki, E. P., DeSantis, T. Z., Probst, A., … Hugenholtz, P. (2012). An improved Greengenes taxonomy with explicit ranks for ecological and evolutionary analyses of bacteria and archaea. *ISME Journal, 6*(3), 610–618. https://doi.org/10.1038/ismej.2011.139

Mengucci, C., Nissen, L., Picone, G., Malpuech-Brugère, C., Orfila, C., Ricciardiello, L., … Gianotti, A. (2022). K-clique multiomics framework: A novel protocol to decipher the role of gut microbiota communities in nutritional intervention trials. *Metabolites, 12*(8), 736. https://doi.org/10.3390/metabo12080736

Minekus, M., Alminger, M., Alvito, P., Ballance, S., Bohn, T., Bourlieu, C., … Brodkorb, A. (2014). A standardised static *in vitro* digestion method suitable for food - an international consensus. *Food & Function, 5*(6), 1113–1124. https://doi.org/10.1039/c3fo60702j

Nagao-Kitamoto, H., & Kamada, N. (2017). Host-microbial cross-talk in inflammatory bowel disease. *Immune Network, 17*(1), 1–12.

Nissen, L., Casciano, F., Babini, E., & Gianotti, A. (2023). Beneficial metabolic transformations and prebiotic potential of hemp bran and its alcalase hydrolysate, after colonic fermentation in a gut model. *Scientific Reports, 13*(1), 1552. https://doi.org/10.1038/s41598-023-27726-w

Nissen, L., Casciano, F., Chiarello, E., Di Nunzio, M., Bordoni, A., & Gianotti, A. (2021). Colonic *in vitro* model assessment of the prebiotic potential of bread fortified with polyphenols rich olive fiber. *Nutrients, 13*(3), Article 787. https://doi.org/10.3390/nu13030787

Nissen, L., Cattivelli, A., Casciano, F., Gianotti, A., & Tagliazucchi, D. (2022). Roasting and frying modulate the phenolic profile of dark purple eggplant and differently change the colon microbiota and phenolic metabolites after *in vitro* digestion and fermentation in a gut model. *Food Research International, 160*, Article 111702. https://doi.org/10.1016/j.foodres.2022.111702

Nissen, L., di Carlo, E., & Gianotti, A. (2020). Prebiotic potential of hemp blended drinks fermented by probiotics. *Food Research International, 131*, Article 109029. https://doi.org/10.1016/j.foodres.2020.109029

Nissen, L., Samaei, S. P., Babini, E., & Gianotti, A. (2020). Gluten free sourdough bread enriched with cricket flour for protein fortification: Antioxidant improvement and volatilome characterization. *Food Chemistry, 333*, Article 127410.

Nissen, L., Valerii, M. C., Spisni, E., Casciano, F., & Gianotti, A. (2021). Multiunit *in vitro* colon model for the evaluation of prebiotic potential of a fiber plus D-limonene food supplement. *Foods, 10*(10), Article 2371. https://doi.org/10.3390/foods10102371

Oba, S., Sunagawa, T., Tanihiro, R., Awashima, K., Sugiyama, H., Odani, T., … Sasaki, K. (2020). Prebiotic effects of yeast mannan, which selectively promotes *Bacteroides thetaiotaomicron* and *Bacteroides ovatus* in a human colonic microbiota model. *Scientific Reports, 10*(1), 17351. https://doi.org/10.1038/s41598-020-74379-0

Powles, S. T., Gallagher, K. I., Chong, L. W., Alexander, J. L., Mullish, B. H., Hicks, L. C., … Orchard, T. R. (2022). Effects of bowel preparation on intestinal bacterial associated urine and faecal metabolites and the associated faecal microbiome. *BMC gastroenterology, 22*(1), 1–9.

Rizzello, F., Ricci, C., Scandella, M., Cavazza, E., Giovanardi, E., Valerii, M. C., … Spisni, E. (2018). Dietary geraniol ameliorates intestinal dysbiosis and relieves symptoms in irritable bowel syndrome patients: A pilot study. *BMC Complementary and Alternative Medicine, 18*, 1–11.

Roager, H. M., & Licht, T. R. (2018). Microbial tryptophan catabolites in health and disease. *Nature Communications, 9*, 3294.

Rowan, F., Docherty, N. G., Murphy, M., Murphy, B., Calvin Coffey, J., & O'Connell, P. R. (2010). *Desulfovibrio* bacterial species are increased in ulcerative colitis. *Disease Colon Rectum, 53*(11), 1530–1536. https://doi.org/10.1007/DCR.0b013e3181f1e620

Scherf, K. A. (2019). Immunoreactive cereal proteins in wheat allergy, non-celiac gluten/wheat sensitivity (NCGS) and celiac disease. *Current Opinion in Food Science, 25*, 35–41.

Selma, M. V., Espin, J. C., & Tomas-Barberan, F. A. (2009). Interaction between phenolics and gut microbiota: Role in human health. *Journal of Agricultural and Food Chemistry, 57*(15), 6485–6501.

Tamargo, A., Cueva, C., Silva, M., Molinero, N., Miralles, B., Bartolomé, B., & Moreno-Arribas, M. V. (2022). Gastrointestinal co-digestion of wine polyphenols with glucose/whey proteins affects their bioaccessibility and impact on colonic microbiota. *Food Research International, 155*, Article 111010. https://doi.org/10.1016/j.foodres.2022.111010

Tanner, S. A., Zihler Berner, A., Rigozzi, E., Grattepanche, F., Chassard, C., & Lacroix, C. (2014). In vitro continuous fermentation model (PolyFermS) of the swine proximal colon for simultaneous testing on the same gut microbiota. *PLoS One1, 9*(4), Article e94123. https://doi.org/10.1371/journal.pone.0094123

Taslimi, P., Sujayev, A., Karaman, M., Maharramova, G., Sadeghian, N., Osmanova, S., … Gulcin, İ. (2020). N-Substituted pyrimidinethione and acetophenone derivatives as a new therapeutic approach in diabetes. *Archiv der Pharmazie, 353*(9), Article e2000075. https://doi.org/10.1002/ardp.202000075

Traore, S. I., Khelaifia, S., Armstrong, N., Lagier, J. C., & Raoult, D. (2019). Isolation and culture of *Methanobrevibacter smithii* by co-culture with hydrogen-producing bacteria on agar plates. *Clinical Microbiology Infection, 25*(12), 1561.e1–1561.e5.

Tsitko, I., Wiik-Miettinen, F., Mattila, O., Rosa-Sibakov, N., Seppänen-Laakso, T., Maukonen, J., Nordlund, E., & Saarela, M. (2019). A small *in vitro* fermentation model for screening the gut microbiota effects of different fiber preparations. *International Journal Molecular Science, 20*(8), Article 1925. https://doi.org/10.3390/ijms20081925

Vázquez-Baeza, Y., Pirrung, M., Gonzalez, A., & Knight, R. (2013). EMPeror: A tool for visualizing high-throughput microbial community data. *GigaScience, 2*(1), 2047–2217.

Von Aulock, S. (2019). Is there an end in sight for animal testing? Can organ-on-a-chip replace animal use in safety testing with advanced human-focused approaches? *ALTEX, 36*(1), 142–144. 10.14573/altex.1812121.

Wang, Q., Garrity, G. M., Tiedje, J. M., & Cole, J. R. (2007). Naive Bayesian classifier for rapid assignment of rRNA sequences into the new bacterial taxonomy. *Applied Environmental Microbiology, 73*(16), 5261–5267. https://doi.org/10.1128/AEM.00062-07

Wang, X., Gibson, G. R., Sailer, M., Theis, S., & Rastall, R. A. (2020). Prebiotics inhibit proteolysis by gut bacteria in a host diet-dependent manner: A three-stage continuous in vitro gut model experiment. *Applied Environmental Microbiology, 86* (10), e02730–e10819. https://doi.org/10.1128/AEM.02730-19

Young, S. J., Liu, Y. H., Lin, Z. D., Ahmed, K., Shiblee, M. D. N. I., Romanuik, S., … Arya, S. (2020). Multi-walled carbon nanotubes decorated with silver nanoparticles for acetone gas sensing at room temperature. *Journal of Electrochemical Society, 167* (16), Article 167519.

Zelante, T., Puccetti, M., Giovagnoli, S., & Romani, L. (2021). Regulation of host physiology and immunity by microbial indole-3-aldehyde. *Current Opinion in Immunology, 70*, 27–32.

Zhang, D., Gong, L., Ding, S., Tian, Y., Jia, C., Liu, D., … Hu, Q. N. (2020). FRCD: A comprehensive food risk component database with molecular scaffold, chemical diversity, toxicity, and biodegradability analysis. *Food Chemistry, 318*, Article 126470. https://doi.org/10.1016/j.foodchem.2020.126470

Zhang, Y., Xu, M., Zhang, X., Hu, Y., & Luan, G. (2022). Application of zein in gluten-free foods: A comprehensive review. *Food Research International*, Article 111722.

Zhou, J., Sun, T., Kang, W., Tang, D., & Feng, Q. (2020). Pathogenic and antimicrobial resistance genes in *Streptococcus oralis* strains revealed by comparative genome analysis. *Genomics, 112*(5), 3783–3793. https://doi.org/10.1016/j.ygeno.2020.04.014